

# International Round-Robin Test of Critical Current of Superconducting Cable Sample

T. Matsushita<sup>1</sup>, M. Kiuchi<sup>2</sup>, T. Masuda<sup>3</sup>, S. Mukoyama, K. Funaki, J. Cho<sup>4</sup>, J. Lu<sup>5</sup>, M. J. Raine<sup>6</sup>, L. Quéval<sup>7</sup>, F. Trillaud<sup>8</sup>, G. Zhang<sup>9</sup>, M. Song<sup>10</sup>, J. Zheng<sup>11</sup>, *Member, IEEE*, Z. Chen<sup>12</sup>, and J. Li<sup>13</sup>

**Abstract**—Ten institutes from six countries participated in an international round-robin test to evaluate the critical current of a superconducting power cable made of Bi-2223 tapes. The cable design featured a two-layer inner core conductor and a single-layer outer shield conductor. The shield layer measured approximately 40 mm in diameter, and the cable length was 2.0 m. To eliminate the influence of resistive voltage drops from current transfer, voltage taps for measurement were positioned at a sufficient distance from the current terminals. The critical current was determined using the resistive method with the electric field criterion of 1.0  $\mu\text{V}/\text{cm}$ . In addition, the  $n$ -value, an optional parameter reflecting the current–voltage ( $I$ – $V$ ) characteristics, was extracted from the  $I$ – $V$  curve within an electric field range of 0.1–1.0  $\mu\text{V}/\text{cm}$ . A detailed uncertainty analysis was conducted for both the critical current and the  $n$ -value. Finally, this article discusses the potential for standardization of the employed resistive measurement method.

**Index Terms**—Critical current, experimental standard deviation,  $n$ -value, round-robin test, superconducting cable.

## I. INTRODUCTION

THE growing threat of global warming due to CO<sub>2</sub> emission is exacerbated by the anticipated surge in electricity consumption from data centers fueled by artificial intelligence advancements. High-temperature superconducting (HTS) power cables offer a promising solution, particularly for data centers, because of their zero power transmission loss in direct current. Extensive research and development efforts have been undertaken on HTS cables [1], [2], [3], [4], [5], [6], [7], [8], [9], [10], [11], [12], [13], [14], alongside numerous demonstration projects to identify real-word challenges [15], [16], [17], [18], [19], [20], [21], [22].

Recognizing the need for standardized testing procedures during ongoing in-grid deployments, Working Group B1.31 of the International Council on Large Scale Electric Systems published a report in 2013 recommending various testing methods for superconducting cables, including critical current measurement [23]. This recommendation was followed by the International Electrotechnical Commission’s publication of an international standard in 2018 for testing methods and requirements on HTS-ac power cables and their accessories. The standard also highlighted the need for a standardized dc critical current test method [24]. A three-year (2018–2021) Japanese project aimed to address challenges in standardizing a critical current test method and carried out national round-robin testing using two Bi-2223 superconducting cables. An additional parameter characterizing the cable, the  $n$ -value, was also measured. Three Japanese institutions participated in this initial test, and the results of the test are reported in [25].

The domestic test demonstrated the suitability of the employed resistive measurement method as a standard, with experimental standard deviations for critical current ranging from 0.2 to 1.3% for both the cable layers. However, the limited number of participants necessitated an expanded international test. The COVID-19 pandemic in 2020 initially delayed the international round-robin test due to the logistics in shipping the cable. In 2021, the sample cable B from the domestic test was sent internationally, but unfortunately, it was damaged in the test and needed replacement. Finally, in 2022 and 2023, an international round-robin test using the sample cable C was successfully conducted with participation from ten institutes across six countries: Sumitomo Electric Industries, Ltd. (Japan), Furukawa Electric

Manuscript received 15 March 2024; revised 6 June 2024 and 26 June 2024; accepted 25 July 2024. Date of publication 5 August 2024; date of current version 27 August 2024. The work of J. Lu was performed at the National High Magnetic Field Laboratory, which is supported by National Science Foundation Cooperative Agreement No. DMR-1644779, and the State of Florida. The work of L. Quéval was supported in part by the French Organization for Standardization AFNOR/UF TC90 and in part by the SuperRail project, funded by the French Government as part of the “Plan de Relance” and the “Programme d’investissements d’avenir.” (Corresponding author: M. Kiuchi.)

T. Matsushita and M. Kiuchi are with the Kyushu Institute of Technology, Iizuka 820-8502, Japan (e-mail: matsushita391teruo@outlook.jp; kiuchi@phys.kyutech.ac.jp).

T. Masuda is with Sumitomo Electric Industries, Ltd., Konohana-ku 554-0024, Japan (e-mail: masuda-takato@sei.co.jp).

S. Mukoyama is with Furukawa Electric Company, Hiratsuka 254-0016, Japan (e-mail: tc90mukoyama@jema.jp).

K. Funaki is with Kyushu University, Nishi-ku 819-0395, Japan (e-mail: funaki.kazuo.681@m.kyushu-u.ac.jp).

J. Cho is with the Korea Electrotechnology Research Institute, Changwon 511543, South Korea (e-mail: jwcho@keri.re.kr).

J. Lu is with National High Magnetic Field Laboratory, Tallahassee, FL 32310 USA (e-mail: junlu@magnet.fsu.edu).

M. J. Raine is with Durham University, Durham DH1 3LE, U.K. (e-mail: m.j.raine@durham.ac.uk).

L. Quéval is with the University of Paris-Saclay, 91190 Paris, France (e-mail: loic.queval@geeps.centralesupelec.fr).

F. Trillaud is with the Instituto de Ingeniería, Universidad Nacional Autónoma de México, Ciudad de México 04510, México (e-mail: ftrillaudp@ii.unam.mx).

G. Zhang is with the Institute of Electrical Engineering, Chinese Academy of Sciences, Beijing 100190, China (e-mail: gmzhang@mail.iee.ac.cn).

M. Song is with Guangdong Power Grid Corporation, Guangzhou 510630, China (e-mail: 5487100@qq.com).

J. Zheng is with the Institute of Plasma Physics, Chinese Academy of Sciences, Hefei 230031, China (e-mail: jxzheng@ipp.ac.cn).

Z. Chen is with Shanghai International Superconductor Technology Company, Ltd., Shanghai 200444, China (e-mail: chenzhijue@secri.com).

J. Li is with the Institute of Physics, Chinese Academy of Sciences, Beijing 100190, China (e-mail: lijie@iphy.ac.cn).

Color versions of one or more figures in this article are available at <https://doi.org/10.1109/TASC.2024.3438251>.

Digital Object Identifier 10.1109/TASC.2024.3438251



Fig. 1. Measured sample cable. The silver part in the central area is the outer shield conductor, and two copper plates at both the ends are attached to the inner core conductor.

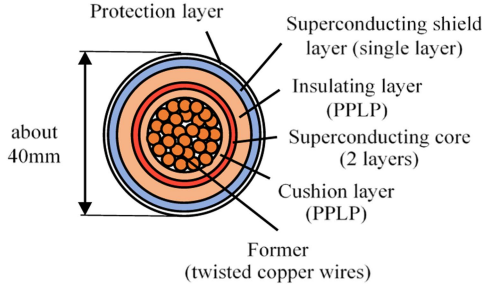


Fig. 2. Cross section of the cable.

TABLE I  
STRUCTURE OF THE SAMPLE CABLE

	Layer	No. of tapes	Winding	Pitch [mm]	Diameter [mm]
Core	1st	14	S	250	22
	2nd	15	Z	320	23
Shield	Single	26	S	600	40

Company (Japan), Kyushu Institute of Technology (Japan), Korea Electrotechnology Research Institute (Korea), National High Magnetic Field Laboratory (USA), Durham University (U.K.), University Paris-Saclay (France), Guangdong Power Grid Company Ltd. (China), Institute of Plasma Physics (China), and Shanghai International Superconductor Technology Company Ltd. (China).

## II. EXPERIMENTS

The superconducting cable C, wound using Bi-2223 tapes of 4.0 mm in width, was used for the measurements. Fig. 1 represents the overall structure of the cable, and a cross-sectional diagram detailing the internal arrangement is shown in Fig. 2. The cable featured the core conductor composed of two superconducting tape layers and the single-layer outer shield conductor. The total length was 2.0 m. The inner core and outer shield were separated by an insulator layer for electrical insulation. The solid structure was employed to ensure safe transportation to participating institutes abroad. Table I provides a detailed breakdown of the cable structure. “S” and “Z” denote the right- and left-hand twist directions of the tapes within each layer, respectively. The number of tapes used for the first and second layers of the inner core was 14 and 15, respectively, while the outer shield utilizes 26 tapes. The current terminals, constructed from copper blocks, were attached to the 4.25-mm-thick copper sheath encasing the superconducting tapes.

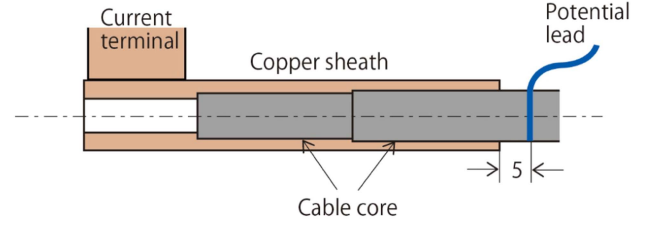


Fig. 3. Arrangement around the current terminal of the cable core.

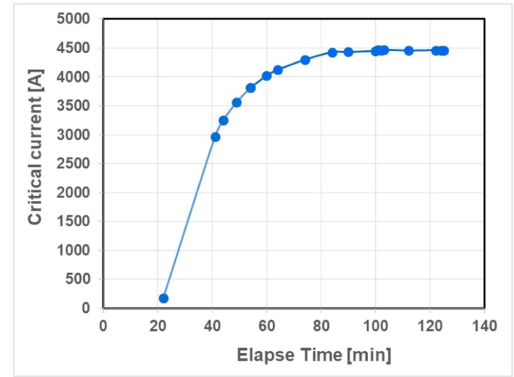


Fig. 4. Observed critical current of the cable core as a function of the time after immersing the cable in the liquid nitrogen bath.

The voltage taps were peripherally attached on every superconducting tape of the surface layer for both the inner core and the outer shield, as indicated by the blue line in Fig. 3 [26]. The distance maintains 5 mm from the edge of the copper sheath to eliminate the influence of the resistive voltage due to current transfer [26]. Although the voltage taps are not directly connected to the inner layer of the core, the electric potential of each layer is considered to be equivalent between the two layers due to the absence of current transfer, as will be shown later.

Measurements were conducted on both the inner core and the outer shield of the sample cable. Achieving a stable operational state necessitated sufficient cooling in liquid nitrogen. Fig. 4 displays the results of a preliminary test on the critical current of the inner core as a function of time after immersion in the liquid nitrogen bath. This test demonstrates the time required for the inner core and the outer shield to reach the liquid nitrogen temperature, which is approximately 90 and 40 min, respectively. Each participating institute employed a current sweep rate optimized for their measurement setup, ranging from a dc (0 A/s) condition for a stepwise change to a maximum around 300 A/s. Fig. 5(a) and (b) depicts the current versus electric field curves obtained by the High Magnetic Field Laboratory in the USA for the inner core and the outer shield, respectively, at a sweep rate of 36 A/s. Resistive voltage was not observed, and we can conclude that no current transfer occurred [26].

The critical current at the reference temperature of 77.30 K, denoted as  $I_c(0)$ , was determined from the measured critical current using the following equation [27]:

$$\frac{I_c(\Delta T)}{I_c(0)} = 1 - 0.05082\Delta T \quad (1)$$

TABLE II  
 $I_c$  VALUE OF (A) THE INNER CORE AND (B) THE OUTER SHIELD

(a) Institute	Measured Value [A]			Average [A]	$s_i$ [A]	$s_{ri}$ [%]
	1st	2nd	3rd			
Sumitomo	4337	4337	4347	4340	6	0.1
Furukawa	4389	4358	4419	4389	31	0.7
Kyushu I. T.	4340	4343	4337	4340	3	0.1
KERI	4292	4295	4299	4295	4	0.1
NHMFL	4307	4305	4307	4306	1	0.0
Durham U.	4387	4385	4386	4386	1	0.0
U. Paris-Saclay	4380	4389	4393	4397	7	0.2
Guangdon P. G.	4315	4329	4303	4316	13	0.3
I. Plasma Phys.	4320	4318	4325	4321	4	0.1
Shanghai I. S. T.	4281	4286	4292	4286	6	0.1

(b) Institute	Measured Value [A]			Average [A]	$s_i$ [A]	$s_{ri}$ [%]
	1st	2nd	3rd			
Sumitomo	3946	3966	3976	3963	15	0.4
Furukawa	3990	3991	3998	3993	4	0.1
Kyushu I. T.	4060	4074	4069	4068	7	0.2
KERI	4014	4023	4027	4021	7	0.2
NHMFL	4050	4059	4058	4056	5	0.1
Durham U.	4140	4140	4148	4143	5	0.1
U. Paris-Saclay	4088	4117	4118	4108	17	0.4
Guangdon P. G.	4062	4075	4085	4074	12	0.3
I. Plasma Phys.	4010	4030	4040	4025	15	0.4
Shanghai I. S. T.	4039	4042	4039	4040	2	0.0

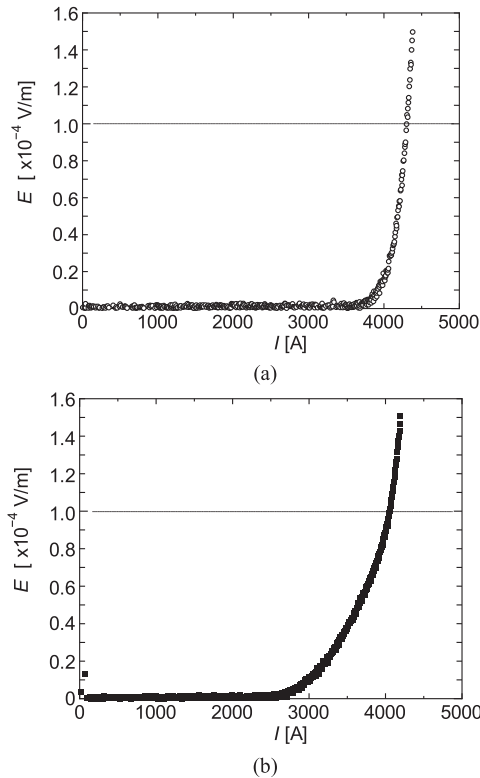


Fig. 5. Current versus electric field curve of (a) cable core and (b) shield in the National High Magnetic Field Laboratory in the USA.

where  $\Delta T = T - 77.30$ . The  $n$ -value was additionally measured within the electric field range of 0.1–1.0  $\mu\text{V}/\text{cm}$ . Each measurement was repeated three times.

### III. RESULTS AND DISCUSSION

Table II summarizes the critical current measurements for the inner core and the outer shield obtained by each participating

institute. The relative experimental standard deviations ( $s_{ri}$ ) are generally low across all the institutes, with most values falling below 0.4%. This level of deviation is likely attributable to the uncertainty associated with the instruments used in the experiment. Similarly, Table III shows that the relative experimental standard deviations for the  $n$ -value are also low across all the institutes.

Table IV presents the critical currents and  $n$ -values for the inner core and the outer shield as determined by all the participants. The  $n$ -value obtained for the outer shield by French institute exhibits a significant deviation. This can be attributed to the fitting process using the  $n$ -value model within an electric field range exceeding 1.0  $\mu\text{V}/\text{cm}$ . Consequently, this value was excluded from the statistical analysis. Although larger than the values observed within individual institutes, the overall relative experimental standard deviations remained acceptable, reaching 0.90% and 1.3% for the inner core and the outer shield, respectively. Conversely, the experimental standard deviations for the  $n$ -value were considerably higher, reaching 11.1% and 15.4% for the inner core and the outer shield, respectively. These values are consistent with the results reported in the previous domestic round-robin test [25].

We, now, investigate the uncertainty associated with the critical current measurement. Based on the  $n$ -value model, the critical current can be expressed as

$$I_c = I_0(T_0) = \left[ I(V) \left( \frac{E_{cl}}{V} \right)^{1/n} \right]_{V=E_{cl}} \quad (2)$$

where  $E_c = 1.0 \times 10^{-4} \text{ V}/\text{m}$  is the electric field criterion and  $l$  denotes the distance between the voltage taps. Assuming a uniform distribution for the deviation of the measured temperature with a distribution width of  $2\delta T$ , the relative standard uncertainty stemming from temperature measurement using (1)

TABLE III  
*n*-VALUE OF (A) THE INNER CORE AND (B) THE OUTER SHIELD

(a) Institute	Measured Value			Average	$s_i$	$s_{ri}$ [%]
	1st	2nd	3rd			
Sumitomo	20.0	21.0	21.0	20.7	0.6	2.8
Furukawa	21.3	22.1	22.2	21.9	0.5	2.3
Kyushu I. T.	20.0	21.0	20.2	20.3	0.6	2.9
KERI	20.3	20.9	21.9	21.0	0.8	3.8
NHMFL	25.8	25.6	25.9	25.8	0.1	0.5
Durham U.	25.1	26.3	25.7	25.7	0.6	2.3
U. Paris-Saclay	24.2	22.3	21.9	22.8	1.2	5.3
Guangdon P. G.	18.9	19.2	18.9	19.0	0.2	1.1
I. Plasma Phys.	20.9	20.0	20.3	20.4	0.8	3.9
Shanghai I. S. T.	19.4	19.1	19.7	19.4	0.3	1.5

(b) Institute	Measured Value			Average	$s_i$	$s_{ri}$ [%]
	1st	2nd	3rd			
Sumitomo	7.0	7.0	7.0	7.0	0	0
Furukawa	8.2	8.2	8.5	8.3	0.2	2.1
Kyushu I. T.	7.6	7.5	7.6	7.6	0.1	0.9
KERI	9.9	9.6	9.5	9.7	0.2	2.1
NHMFL	7.3	7.3	7.3	7.3	0	0
Durham U.	7.4	7.6	7.3	7.4	0.1	2.1
U. Paris-Saclay	11.0	12.7	12.7	12.1	1.0	8.3
Guangdon P. G.	6.7	6.5	6.4	6.5	0.2	3.1
I. Plasma Phys.	9.4	9.6	9.7	9.6	0.2	2.1
Shanghai I. S. T.	6.8	6.7	6.7	6.7	0.1	1.5

TABLE IV  
 CRITICAL CURRENT AND *n*-VALUE

Institute	Inner core		Outer shield	
	$I_c$ [A]	<i>n</i> -value	$I_c$ [A]	<i>n</i> -value
Sumitomo	4340	20.7	3963	7.0
Furukawa	4389	21.9	3993	8.3
Kyushu I. T.	4340	20.3	4068	7.6
KERI	4295	21.0	4021	9.7
NHMFL	4306	25.8	4056	7.3
Durham U.	4386	25.7	4143	7.4
U. Paris-Saclay	4387	22.8	4108	(12.1)*
Guangdon P. G.	4316	19.0	4074	6.5
I. Plasma Phys.	4321	20.4	4027	9.6
Shanghai I. S. T.	4286	19.4	4040	6.7
Average	4337	21.7	4049	7.8
$s$	39	2.4	53	1.2
$s_r$ [%]	0.90	11.1	1.3	15.4

\*The *n*-value was measured in the electric field range above 1.0  $\mu\text{V}/\text{cm}$ , and this value is not included in the statistical analysis.

can be calculated as

$$u_{rT} = \frac{0.05082\delta T}{\sqrt{3}} \simeq 0.029\delta T. \quad (3)$$

The relative standard uncertainties of the critical current arising from the current source, voltmeter, and distance between the voltage taps can be expressed as

$$u_{rI} = \frac{\delta I}{\sqrt{3}I}, \quad u_{rV} = \frac{\delta V}{\sqrt{3nV}}, \quad u_{rl} = \frac{\delta l}{\sqrt{3nl}} \quad (4)$$

where  $\pm\delta I/I$ ,  $\pm\delta V/V$ , and  $\pm\delta l/l$  represent the allowable ranges of relative deviation for the current, voltage, and distance between the voltage taps, respectively. Then, the relative uncertainty of the critical current is

$$u_r = (u_{rT}^2 + u_{rI}^2 + u_{rV}^2 + u_{rl}^2)^{1/2}. \quad (5)$$

First, we discuss the experimental standard deviation observed within each institute. Since three measurements are typically performed in a relatively short period, the temperature variation is likely minimal, even if the absolute temperature is unknown. Therefore, the temperature correction remains consistent across the three measurements. Consequently, the uncertainty  $u_{rT}$  due to short-term temperature fluctuations can be disregarded. Under this assumption, the relative standard uncertainty simplifies to

$$u_r = \left[ \frac{1}{3} \left( \frac{\delta I}{I} \right)^2 + \frac{1}{3n^2} \left( \frac{\delta V}{V} \right)^2 + \frac{1}{3n^2} \left( \frac{\delta l}{l} \right)^2 \right]^{1/2}. \quad (6)$$

Given the large value of *n*, the terms associated with the voltage and distance uncertainties can be neglected. Typically,

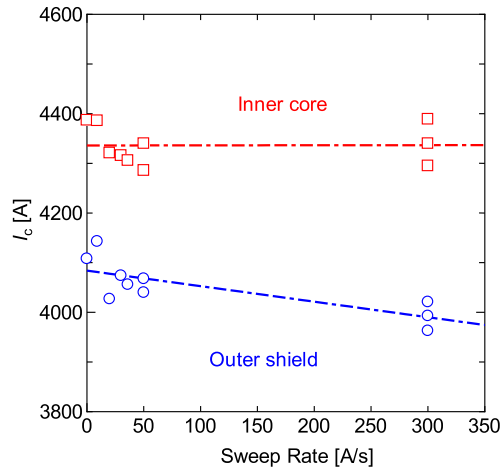


Fig. 6. Current sweep-rate dependence of the critical current.

the allowable deviation for the current measurement is assumed to be 0.5% ( $\delta I/I = 0.005$ ); substituting this value into (6) yields an uncertainty of approximately  $u_r \simeq 0.003$  (0.3%). This value originally represents the relative experimental standard deviation among the participating institutes. Since the relative experimental standard deviations arising from repeated measurements within each institute are expected to be smaller than those among the institutes, it is reasonable that most values of  $s_{ri}$  are smaller than  $u_r$ , as evident in Table II.

Now, we discuss the relative experimental standard deviation across all the institutes. In this case, we can again safely neglect the relative uncertainties associated with voltage and distance measurements. Therefore, the relative uncertainty becomes

$$u_r = \left[ (0.029\delta T)^2 + \frac{1}{3} \left( \frac{\delta I}{I} \right)^2 \right]^{1/2}. \quad (7)$$

Assuming a half-width of temperature distribution of  $\delta T = 0.25$  K, which corresponds to the uncertainty of the temperature of 0.14 K, we have  $u_r = 0.008$  (0.80%). This value is close to the obtained experimental standard deviation of 0.90% for the inner core. However, the experimental standard deviation for the outer shield is larger than that of the inner core, which aligns with the findings of the domestic round-robin test [25]. This suggests an additional source of standard deviation specific to the outer shield measurements. This discrepancy could potentially be linked to anomalies in the  $E-I$  characteristic behavior within the electric field range below  $1.0 \mu\text{V}/\text{cm}$ , which also explains the lower  $n$ -value observed for the outer shield.

The observed anomaly in the outer shield is hypothesized to be caused by a current transfer mechanism. Damaged superconducting tapes within the outer shield may transfer current to intact tapes, inducing an additional flux flow voltage. This implies that the anomaly is dependent on the sweep rate of the applied current  $\dot{I}$ . As shown in Fig. 6, the critical current of the outer shield exhibits a significant dependence on  $\dot{I}$ , whereas the inner core does not. Using the least squares method, this dependence is expressed as

$$I_c = 4084 \left( 1 - 0.766 \times 10^{-4} \dot{I} \right) \quad (8)$$

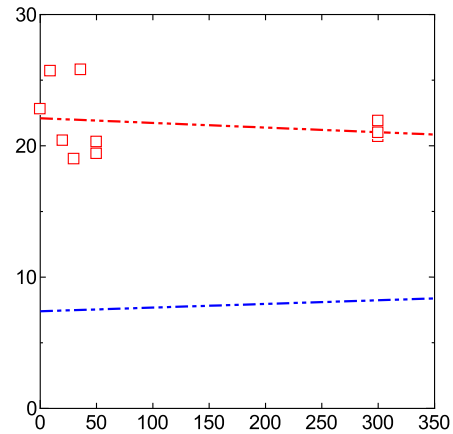


Fig. 7. Current sweep-rate dependence of the  $n$ -value.

for the shield and

$$I_c = 4336 \left( 1 + 0.456 \times 10^{-6} \dot{I} \right) \quad (9)$$

for the core. Accounting for the sweep-rate dependence, the experimental standard deviations and their relative values for each conductor are presented in Table V. Notably, the relative experimental standard deviations are comparable for the two conductors.

For the  $n$ -value, the experimental standard deviation ( $s_i$ ) within each institute is similar for both the inner core and outer shield conductors. However, it is significantly larger than that observed for the critical current. This is likely due to the influence of noise voltage around  $0.1 \mu\text{V}/\text{cm}$ . The interinstitute standard deviation ( $s$ ) for the  $n$ -value is considerably larger than the intrainstitute standard deviations ( $s_i$ ). Similar to the critical current measurement, this is likely caused by uncertainties in temperature measurement and variations in the methods used by different institutes to determine the  $n$ -value. We further investigated the effect of the current sweep rate on the  $n$ -value, yielding the following relationships:

$$n = 22.1 \left( 1 - 0.160 \times 10^{-3} \dot{I} \right) \quad (10)$$

for the core and

$$n = 7.4 \left( 1 + 0.377 \times 10^{-3} \dot{I} \right) \quad (11)$$

for the shield (see Fig. 7). The observed increase in the  $n$ -value of the outer shield with increasing sweep rate correlates with the decrease in the critical current. Both phenomena can be attributed to the anomalous voltage increase. In contrast, the absence of such an anomaly in the inner core results in minimal changes to both the critical current and  $n$ -value. Table V also includes the compensated results for the  $n$ -value.

The results clearly demonstrate a significant difference in the  $n$ -value between the inner core and the outer shield. While the  $n$ -value of the outer shield aligns with values typically observed in short samples, the  $n$ -value of the inner core is considerably higher. This is thought to be a consequence of the more rapid temperature rise within the inner core during the resistive state, due to its limited contact with liquid nitrogen [25].

TABLE V

CHANGE IN THE EXPERIMENTAL STANDARD DEVIATIONS AND THE RELATIVE VALUES OF THE CRITICAL CURRENT AND  $n$ -VALUE DUE TO THE COMPENSATION OF THE EFFECT OF THE CURRENT SWEEP RATE

Compensation	Inner core				Outer shield			
	$I_c$		$n$		$I_c$		$n$	
	$s$ [A]	$s_r$ [%]	$s$	$s_r$ [%]	$s$ [A]	$s_r$ [%]	$s$	$s_r$ [%]
Without	39	0.9	2.4	11.1	53	1.3	1.2	15.4
With	39	0.9	2.3	10.7	33	0.8	1.1	14.1

Based on the preceding discussion, establishing a recommended range for the current sweep rate during measurement might be considered. However, such a restriction would likely hinder the adoption of the proposed method, as optimal experimental condition may vary across different institutes. Therefore, we propose to refrain from specifying a recommended sweep rate.

The results obtained for both the inner and outer conductors suggest that the resistive method employed in the round-robin test is a suitable candidate for a standardized method to determine the critical current of superconducting cables. A target relative combined uncertainty (target uncertainty) of 3% with a coverage factor  $k = 2$  (corresponding to approximately 96% confidence within the uncertainty range) appears achievable. As shown in Table V, all the measured values fall the range of  $2 u_r$  for the inner and outer conductors. Conversely, we believe that further investigation is necessary to establish a standardized measurement method for the  $n$ -value of superconducting cables.

#### IV. CONCLUSION

The international round-robin test for critical current measurement of a Bi-2223 superconducting power cable was successfully completed. The achieved experimental relative standard deviations for the critical current at 77.30 K were 0.90% and 1.3% for the inner and outer conductors, respectively. Uncertainty analysis revealed that the primary contributor to the inter-institute experimental standard deviation was the uncertainty in temperature during the experiment. These findings support that the suitability of the resistive method can be recommended as a standardized testing procedure, aiming for a target uncertainty of 3% with a coverage factor of  $k = 2$ . Notably, all the measured critical current values for both the conductors were within the  $\pm 3\%$  uncertainty range.

However, the experimental relative standard deviations for the  $n$ -value were significantly higher than those observed for the critical current, reaching 11.1% and 23.2% for the inner and outer conductors, respectively. This highlights the need for further investigation to establish a standardized measurement method for the  $n$ -value of superconducting cables.

#### REFERENCES

- [1] L. Y. Xiao et al., "Development of HTS AC power transmission cables," *IEEE Trans. Appl. Supercond.*, vol. 17, no. 2, pp. 1652–1655, Jun. 2007.
- [2] J. F. Maguire et al., "Development and demonstration of a HTS power cable to operate in the long island power authority transmission grid," *IEEE Trans. Appl. Supercond.*, vol. 17, no. 2, pp. 2034–2037, Jun. 2007.
- [3] C. S. Weber, R. Lee, S. Ringo, T. Masuda, H. Yumura, and J. Moscovic, "Testing and demonstration results of the 350 m long HTS cable system installed in Albany, NY," *IEEE Trans. Appl. Supercond.*, vol. 17, no. 2, pp. 2038–2042, Jun. 2007.
- [4] S. H. Sohn et al., "The results of installation and preliminary test of 22.9 kV, 50 MVA, 100 m class HTS power cable system at KEPSCO," *IEEE Trans. Appl. Supercond.*, vol. 17, no. 2, pp. 2043–2046, Jun. 2007.
- [5] S. Mukoyama et al., "Study of an YBCO HTS transmission cable system," *Phys. C, Supercond. Appl.*, vol. 463–465, pp. 1150–1153, 2007.
- [6] M. Yagi, S. Mukoyama, N. Amemiya, S. Nagaya, N. Kashima, and Y. Shiohara, "Development of YBCO HTS cable with low AC loss," *Phys. C, Supercond.*, vol. 468, pp. 2037–2040, 2008.
- [7] V. E. Sytnikov et al., "30 m HTS power cable development and witness sample test," *IEEE Trans. Appl. Supercond.*, vol. 19, no. 3, pp. 1702–1705, Jun. 2009.
- [8] J. H. Lim et al., "Performance test of 100 m HTS power cable system," *IEEE Trans. Appl. Supercond.*, vol. 19, no. 3, pp. 1710–1713, Jun. 2009.
- [9] M. Yagi, S. Mukoyama, N. Amemiya, N. Kashima, S. Nagaya, and Y. Shiohara, "Development of a 10 m long 1 kA 66/77 kV YBCO HTS cable with low ac loss and a joint with low electrical resistance," *Supercond. Sci. Technol.*, vol. 22, 2009, Art. no. 085003.
- [10] J. F. Maguire and J. Yuan, "Status of high temperature superconductor cable and fault current limiter projects at American superconductor," *Phys. C, Supercond.*, vol. 469, pp. 874–880, 2009.
- [11] S. Mukoyama et al., "Development of (RE)BCO cables for HTS power transmission lines," *Phys. C, Supercond.*, vol. 469, pp. 1688–1692, 2009.
- [12] S. Vyatkin, M. Kiuchi, E. S. Otabe, and T. Matsushita, "Design of practical superconducting dc power cable with REBCO coated conductors," *IEEE Trans. Appl. Supercond.*, vol. 25, Aug. 2015, Art. no. 6606207.
- [13] T. Kitamura et al., "Development of tri-axial superconducting cable system for type test," *J. Phys.: Conf. Ser.*, vol. 1054, 2018, Art. no. 012075.
- [14] J. Li, L. Zhang, X. Ye, F. Xia, and Y. Cao, "The research on the current capability and insulating properties of 35 kV/1 kA CD HTS cable witness samples," *Earth Environ. Sci.*, vol. 300, 2019, Art. no. 042020.
- [15] O. Tønnesen et al., "Operation experiments with a 30 kV/100 MVA high temperature superconducting cable system," *Supercond. Sci. Technol.*, vol. 17, 2004, Art. no. S101.
- [16] J. A. Demko et al., "Triaxial HTS cable for the AEP Bixby project," *IEEE Trans. Appl. Supercond.*, vol. 17, no. 2, pp. 2047–2050, Jun. 2007.
- [17] H. Yumura et al., "Phase II of the Albany HTS cable project," *IEEE Trans. Appl. Supercond.*, vol. 19, no. 3, pp. 1698–1701, Jun. 2009.
- [18] T. Masuda et al., "A new HTS cable project in Japan," *IEEE Trans. Appl. Supercond.*, vol. 19, no. 3, pp. 1735–1739, Jun. 2009.
- [19] J. Maguire et al., "Development and demonstration of a fault current limiting HTS cable to be installed in the Con Edison grid," *IEEE Trans. Appl. Supercond.*, vol. 19, no. 3, pp. 1740–1743, Jun. 2009.
- [20] N. Fujiwara, H. Hayashi, S. Nagaya, and Y. Shiohara, "Development of YBCO power devices in Japan," *Phys. C, Supercond. Appl.*, vol. 470, pp. 980–985, 2010.
- [21] M. Yagi et al., "Progress of 275 kV- 3kA YBCO HTS cable," *Phys. C, Supercond. Appl.*, vol. 471, pp. 1274–1278, 2011.
- [22] F. Maguire et al., "Progress and status of a 2G HTS power cable to be installed in the Long Island Power Authority (LIPA) grid," *IEEE Trans. Appl. Supercond.*, vol. 21, no. 3, pp. 961–966, Jun. 2011.
- [23] *Recommendations for Testing of Superconducting Cables*, CIGRE Tech. Brochures 538, 2013.
- [24] *HTS-AC Power Cables and Their Accessories—Test Methods and Requirements*, IEC Standard 63075:2019, 2019.
- [25] T. Matsushita et al., "Round robin test of critical current of superconducting cable," *IEEE Trans. Appl. Supercond.*, vol. 31, no. 5, Aug. 2021, Art. no. 4801004.
- [26] T. Matsushita, M. Kiuchi, G. Nishijima, T. Masuda, S. Mukoyama, and Y. Aoki, "Measurement of critical current of superconducting cable," *Jpn. J. Appl. Phys.*, vol. 60, 2021, Art. no. 123001.
- [27] *Critical Current Measurement—Retained Critical Current After Double Bending at Room Temperature of Ag-Sheathed Bi-2223 Superconducting Wire*, IEC Standard 61788-24, 2nd ed., 2018.